Journal of Materials Chemistry B

ROYAL SOCIETY OF CHEMISTRY

PAPER

View Article Online
View Journal

Cite this: DOI: 10.1039/d5tb00937e

$ONOO^-$ generator constructed with a small molecule photosensitizer and photoinduced NO donor for tumor therapy†

Mengqi Liu,‡ Yuqing Liu,‡ Shaoqi Xie, Jiachen Xia, Tong Sun and Bing Lu *

Multimodal synergistic therapy is an effective means to improve therapeutic outcomes against cancer. Herein, a nanotherapeutic platform for highly efficient photodynamic and NO synergistic therapy through the generation of peroxynitrite ($ONOO^-$) was constructed. Specifically, a new small molecule photosensitizer (**DMATPE-MN**) and photoinduced NO donor (**NTA-CN**) were subtly designed, which displayed similar light absorption in the visible light region. Under the same light irradiation, **DMATPE-MN** and **NTA-CN** can generate a superoxide anion free radical ($O_2^{\bullet-}$) and an NO radical, respectively. Then, **NTA-CN** and **DMATPE-MN** were integrated together into nanocarriers formed from amphiphilic pillararene (**WP5-PEG-OH**) through host–guest and hydrophilic/hydrophobic mechanisms. Exhilaratingly, the NO generation efficiency of **NTA-CN** can be significantly improved after host–guest complexation with **WP5-PEG-OH**. It is even more exciting that the formed nanodrug WP5-NTA/MN can generate $ONOO^-$ after light irradiation. As a result, WP5-NTA/MN exhibited outstanding biocompability and showed high tumor cell lethality under both normoxic and hypoxic conditions. Furthermore, the experimental results *in vivo* also demonstrated its good biosafety and ability to inhibit tumor growth. Thus, we provided a highly promising nanoplatform for multimodal synergistic therapy.

Received 22nd April 2025,
Accepted 8th July 2025

DOI: 10.1039/d5tb00937e

rsc.li/materials-b

Introduction

To date, cancer continues to be one of the leading causes of death worldwide.[1] To address this severe challenge, new therapeutic methods, for example NO therapy and photodynamic therapy (PDT), are springing up.[2–7] NO therapy and PDT cause tumor cell death through the NO radical and reactive oxygen species (ROS), respectively, generated during treatment.[8–10] Both treatments show non-invasiveness and high therapeutic effects. However, the therapeutic effects of NO therapy are limited by NO concentration, and the O_2 content in a tumor cell also has a large effect on the therapeutic outcome of PDT.[11–18] Therefore, a combination of NO therapy and PDT is usually a better choice for improving therapeutic effects against cancer.[19–27] Among them, NO therapy and type I PDT synergistic therapy are particularly notable because it can generate higher levels of cytotoxic peroxynitrite ($ONOO^-$) *via* the reaction between NO radicals and superoxide anion free radicals ($O_2^{\bullet-}$) during the therapeutic process.[28,29] $ONOO^-$ is a multitargeting cytotoxic group, which is capable of reacting with a series of substrates in a tumor cell, such as lipids, DNA and proteins.[30,31] Therefore, the combination of NO therapy and type I PDT can more conveniently maximize the synergistic effects of these two therapeutic methods.

The highly efficient and controllable release of NO by NO donors under external or internal stimulation is key to the

School of Chemistry and Chemical Engineering, Nantong University, Nantong, Jiangsu, 226019, P. R. China. E-mail: 2020028lubing@ntu.edu.cn

† Electronic supplementary information (ESI) available. See DOI: https://doi.org/10.1039/d5tb00937e

‡ These authors contributed equally to this work.

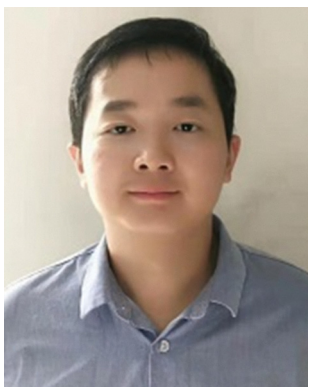

Bing Lu

Bing Lu obtained his BS degree from Soochow University in 2012 and received his PhD from Soochow University in 2017. From 2017 to 2019, he joined Prof. Xiaowei Zhan's group as a postdoctoral fellow. In 2020, he joined the College of Chemistry and Chemical Engineering in Nantong University full time. Currently, he is an associate professor in the College of Chemistry and Chemical Engineering, Nantong University. His research interests are the design and synthesis of functional organic small molecules and their application in biomedicine.

implementation of NO therapy for tumors. To date, various types of NO donors, including *N*-diazeniumdiolates, *S*-nitrosothiols, metal nitrosyls, organic nitrates, furoxans, and *N*-nitrosamines, have been widely used in tumor therapy.[9,15,32,33] The best of them have even been applied in the clinical practice. Nevertheless, their shortcomings cannot be ignored. Some NO donors can spontaneously decompose or release NO prematurely without reaching the symptomatic site. Furthermore, the external or internal factors that can trigger NO release by these NO donors are not unique, making it difficult to achieve a more controllable release of NO. In addition to the above molecules, nitrobenzene compounds, represented by 4-nitro-3-(trifluoromethyl)aniline (NTA), were also early organic NO donors.[34–36] NTA and its derivatives are extremely thermally and chemically stable. The most important thing is that light irradiation is the only stimulation to trigger their NO release, which makes it convenient for their use in NO therapy and PDT synergistic therapy. Although NTA derivatives have been combined with some photosensitizers to build combined NO and PDT therapeutic systems, there are some problems in these systems,[37–40] First, many existing systems suffer from inefficient NO release. It is rather crucial to find appropriate methods to further enhance the NO release efficiency of NTA derivatives. Second, the selected photosensitizers cannot display type I photodynamic activity of photosensitizers, making it difficult to achieve synergistic therapy. Finally, NO donors and photosensitizers have not been subject to specific structural design. It is difficult to make their absorption ranges consistent, which causes difficulty in unifying the light sources for the two treatment modes. Therefore, to date, there have been no reports of NO therapy and type I PDT synergistic therapeutic systems based on NTA derivatives.

In this study, a new NTA derivative, **NTA-CN**, and a small molecule photosensitizer, **DMATPE-MN**, were subtly designed and successfully synthesized (Fig. 1). Through their specific structural design, **NTA-CN** and **DMATPE-MN** displayed the strongest light absorption in similar spectral ranges, which is beneficial for their application under the same light irradiation. Using a single white light source, **NTA-CN** can release NO, and **DMATPE-MN** displayed excellent type I photodynamic activity to generate $O_2^{\bullet-}$. Then, **NTA-CN** and **DMATPE-MN** are loaded into the nanocarriers formed by our previously reported amphiphilic pillararene **WP5-PEG-OH**[41] through host–guest and hydrophilic/hydrophobic mechanisms, respectively.[42–45] **WP5-PEG-OH** can not only provide the nanocarriers with good water solubility for NO donor and photosensitizer but can also significantly improve the photoinduced NO release ability of **NTA-CN** after host–guest complexation. As expected, the formed nanodrug WP5-NTA/MN can generate $ONOO^-$ to complete NO and type I PDT synergistic therapy (Fig. 1). As a result, after exposure to white light, WP5-NTA/MN can effectively kill HeLa cells under both normoxic and hypoxic conditions. Moreover, WP5-NTA/MN still performed well *in vivo*, showing outstanding biosafety and ability to inhibit tumor growth. Therefore, herein, a simple potential NO and PDT synergistic therapeutic system was constructed to achieve highly efficient cancer treatment.

Results and discussion

The methods for synthesising **NTA-CN** and **DMATPE-MN** are summarized in ESI† (Schemes S1 and S2). The intermediates and final products were characterized by nuclear magnetic resonance (NMR) spectra (Fig. S1 and S2, ESI†).

After obtaining **NTA-CN**, we first confirmed its host–guest interaction with **WP5-PEG-OH** *via* NMR and fluorescence titration experiments. As shown in the ^{1}H NMR spectra (Fig. 2), when **WP5-PEG-OH** and **NTA-CN** were mixed at a molar ratio of 1 : 1, the peaks of protons in the aliphatic chain of **NTA-CN** shifted significantly towards high field. These results revealed that the aliphatic chain of **NTA-CN** can penetrate the electron-rich cavity of **WP5-PEG-OH** to form a host–guest complex (**WP5-PEG-OH** ⊃ **NTA-CN**). After complexation of **NTA-CN** with **WP5-PEG-OH**, its fluorescence intensity will be enhanced due to the

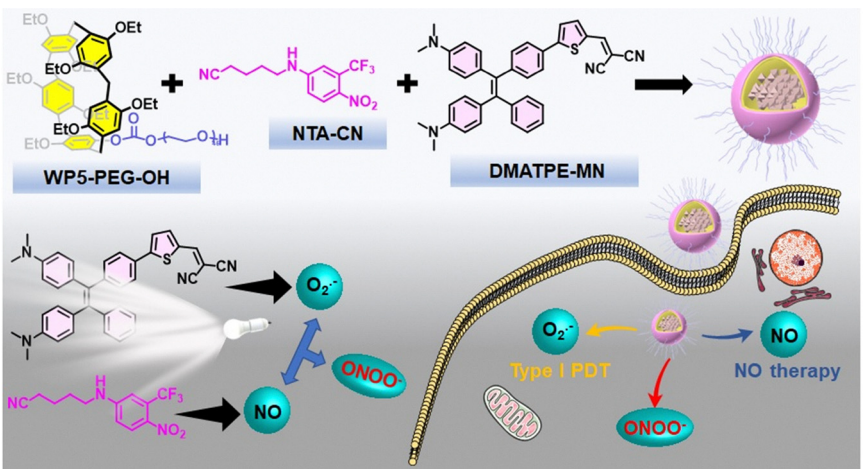

Fig. 1 The chemical structures of **WP5-PEG-OH**, **NTA-CN** and **DMATPE-MN**, and an illustration of their applications in NO and type I PDT synergistic therapy.

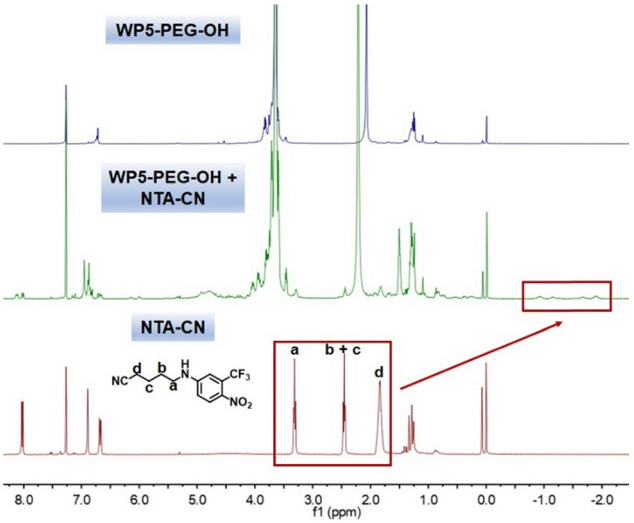

Fig. 2 The ^{1}H NMR spectra of **WP5-PEG-OH** (10 μM), **WP5-PEG-OH** + **NTA-CN** (10 μM + 10 μM) and **NTA-CN** (10 μM) in $CDCl_3$.

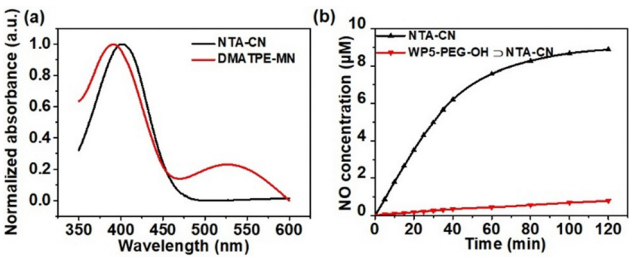

Fig. 3 (a) The light absorption spectra of **NTA-CN** and **DMATPE-MN** in CH_2Cl_2. (b) The NO release profiles of **NTA-CN** (30 μM) and **WP5-PEG-OH** ⊃ **NTA-CN** (30 μM for **NTA-CN**) in H_2O/DMF (9/1).

restricted movement of the side chains of **NTA-CN**. Therefore, the continuously enhanced fluorescent intensity of **NTA-CN** upon addition of **WP5-PEG-OH** can also prove their host–guest behavior (Fig. S4a, ESI†). Their association constant K_a and stoichiometry were calculated to be $(1.27 \pm 0.10) \times 10^4\ M^{-1}$ and 1 : 1, respectively (Fig. S4b, ESI†).

According to the light absorption spectrum of **NTA-CN** (Fig. 3a), white light was used to trigger NO release by **NTA-CN**. It can be seen from Fig. 3b that under light irradiation

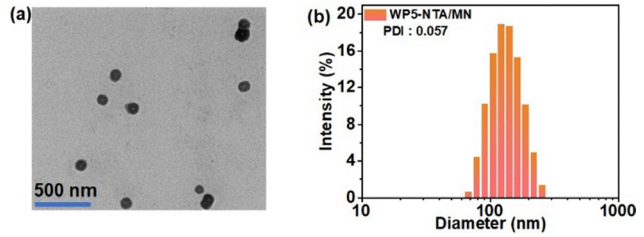

Fig. 5 (a) Transmission electron microscopy images of WP5-NTA/MN. (b) The size distribution of WP5-NTA/MN.

(25 mW cm^{-2}), **NTA-CN** in the absence of **WP5-PEG-OH** showed very poor NO release ability. Surprisingly, after complexation with **WP5-PEG-OH**, the NO release efficiency of **NTA-CN** showed a multifold increase under the same conditions. The enhanced photoactivity of **NTA-CN** after forming a host–guest complex may be attributed to the increased nitro-aromatic twist angle and suppressed intersystem crossing relaxation.[46–49]

Next, the photodynamic activity of **DMATPE-MN** was studied. **DMATPE-MN** displayed strong light absorption between 350 nm and 450 nm, coinciding with that of **NTA-CN** (Fig. 3a). Their similar range of light absorption facilitates their combination to use the same light source for tumor therapy. First, 9,10-anthracenediyl-bis(methylene)dimalonic acid (ABDA) and aminophenyl fluorescein (APF) were used to detect the generation of singlet oxygen ($^1O_2$) and hydroxyl radicals ($^\bullet$OH) of **DMATPE-MN** in CH_2Cl_2 under white light irradiation. The absorbance of ABDA at 380 nm will decrease after reacting with $^1O_2$. Similarly, the fluorescence intensity of APF will increase when meeting $^\bullet$OH. As shown in Fig. S6 (ESI†), Fig. 4a and b, both the changes in absorbance of ABDA and the changes in fluorescence of APF were relatively small, and the changes in the experimental and blank groups were the same. These results demonstrated that **DMATPE-MN** cannot generate $^1O_2$ or $^\bullet$OH after exposure to light. Furthermore, dihydroethidium (DHE) was used to confirm the generation of $O_2^{\bullet-}$ by **DMATPE-MN** under light irradiation. DHE can react with $O_2^{\bullet-}$ to form 2-hydroxyethidium. The fluorescence intensity of 2-hydroxyethidium at 580 nm will increase upon insertion of DNA. It can be seen from Fig. S6 (ESI†) and Fig. 4c that after light irradiation, DHE in the presence of **DMATPE-MN** displayed obviously enhanced fluorescence, suggesting the generation of $O_2^{\bullet-}$ by **DMATPE-MN** under light conditions.

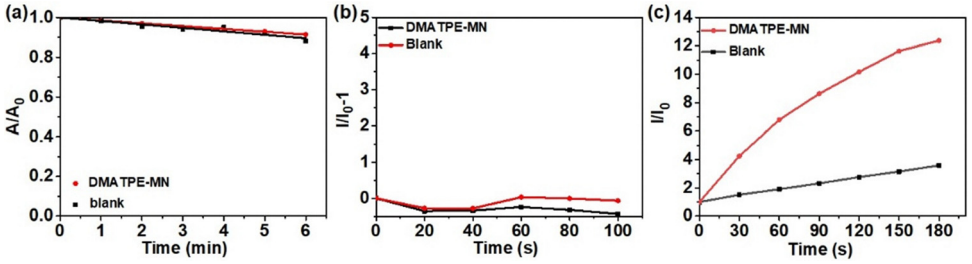

Fig. 4 (a) The changes in absorbance of ABDA at 380 nm in the presence or absence of **DMATPE-MN**. (b) The fluorescence changes in APF at 515 nm in the presence or absence of **DMATPE-MN**. (c) The fluorescence changes in DHE at 580 nm in the presence or absence of **DMATPE-MN** (white light irradiation: 25 mW cm^{-2}).

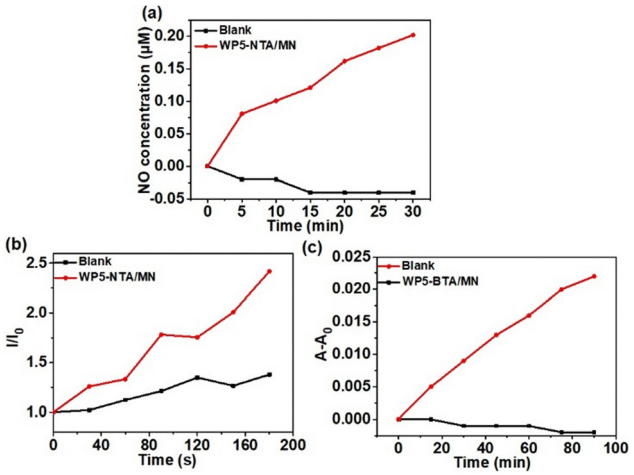

Fig. 6 (a) The NO release profiles of WP5-NTA/MN aqueous solution (200 μg mL^{-1}). (b) The fluorescence changes in DHE at 580 nm in the presence or absence of WP5-NTA/MN aqueous solution (200 μg mL^{-1}). (c) The absorbance changes in LAP at 465 nm in the presence or absence of WP5-NTA/MN aqueous solution (200 μg mL^{-1}).

Encouraged by their outstanding photoactivities, we then successfully integrated **NTA-CN** and **DMATPE-MN** to build a synergistic therapeutic nanoplatform. The formed nanodrug WP5-NTA/MN showed uniform spherical morphology with an average diameter of about 127.4 nm (Fig. 5). Moreover, over a period of time, the sizes of WP5-NTA/MN show no obvious changes, suggesting the good stability of WP5-NTA/MN (Fig. S7, ESI†). The two-dimensional elemental mappings of F and S confirmed the successful loading of **NTA-CN** and **DMATPE-MN** into the nanodrugs (Fig. S8, ESI†).

The NO and $O_2^{\bullet-}$ generation abilities of WP5-NTA/MN were confirmed by the same methods (Fig. 6a and b). Next, a specific probe, LAP, was used to detect the generation of $ONOO^-$ by WP5-NTA/MN under light irradiation (Fig. S9a, ESI†). After reacting with $ONOO^-$, the absorbance of LAP will increase at 465 nm and the absorbance of LAP will decrease at 590 nm. As shown in Fig. 6c and Fig. S9 (ESI†), compared with the blank group, LAP in the presence of WP5-NTA/MN showed more obviously elevated absorbance at 465 nm and reduced

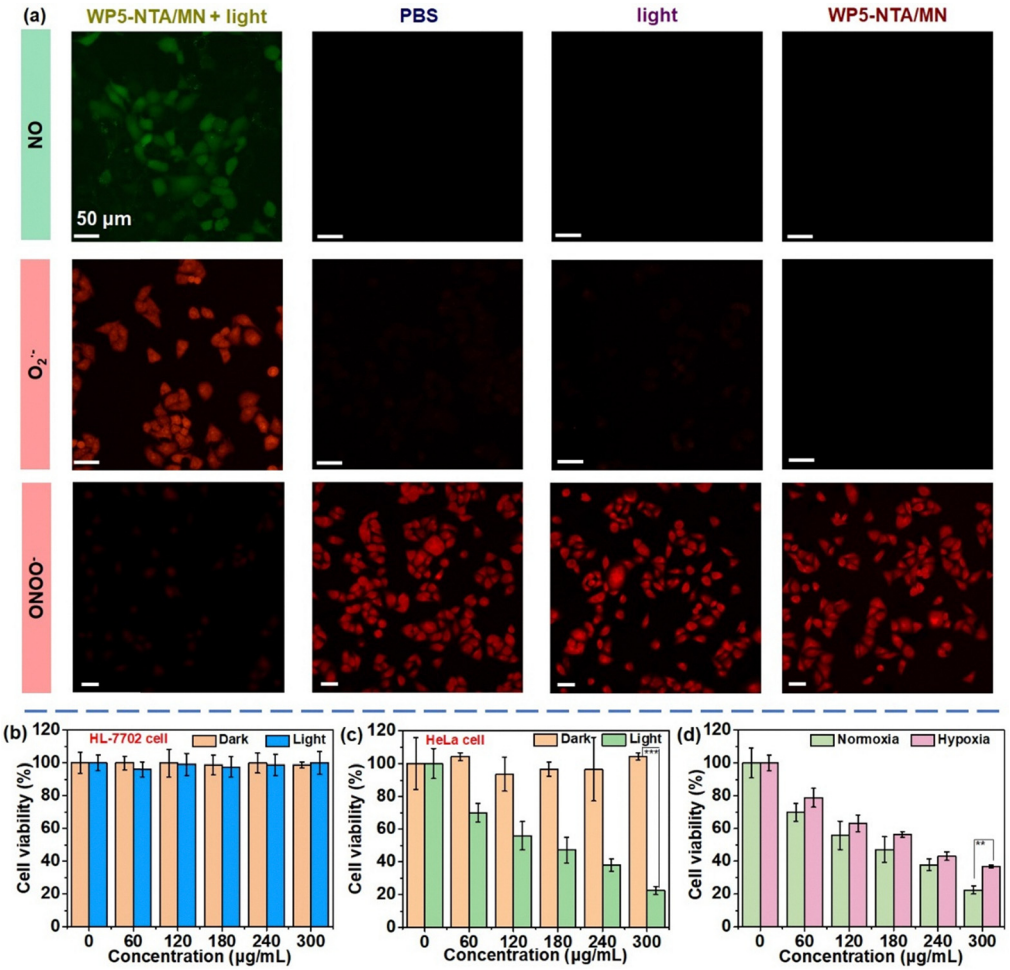

Fig. 7 (a) The detection of NO, $O_2^{\bullet-}$ and $ONOO^-$ in HeLa cells after receiving different treatments using DAF-FM DA, DHE and LAP as fluorescence probes. (b) Viability data for HL-7702 cells incubated with WP5-NTA/MN of different concentrations in the dark or under light conditions, respectively. (c) Viability data for HeLa cells incubated with WP5-NTA/MN of different concentrations in the absence or the presence of light. (d) Viability data for HeLa cells incubated with WP5-NTA/MN of different concentrations under normoxic or hypoxic conditions. Data are presented as mean ± s.d. (n = 6). For all tests, significance is defined as $^{***}p < 0.001$, $^{**}p < 0.01$.

absorbance at 590 nm, indicating the generation of $ONOO^-$ by WP5-NTA/MN under light conditions (25 mW cm^{-2}).

The detection of NO, $O_2^{\bullet-}$ and $ONOO^-$ generated by irradiated WP5-NTA/MN in HeLa cells was then carried out. First, DAF-FM DA was used as a specific probe for the detection of intracellular NO. DAF-FM DA can be hydrolyzed by intracellular esterase to form DAF-FM with only weak fluorescence. DAF-FM can produce strong green fluorescence after reacting with NO. Compared with HeLa cells in control groups, HeLa cells incubated with WP5-NTA/MN displayed bright green fluorescence after light irradiation (Fig. 7a), suggesting the generation of NO by the irradiated WP5-NTA/MN. Similarly, DHE was used as an $O_2^{\bullet-}$ indicator to confirm intracellular $O_2^{\bullet-}$ generation by WP5-NTA/MN under light conditions (Fig. 7a). Finally, LAP was used to detect the generation of $ONOO^-$. After reacting with $ONOO^-$, the fluorescence intensity of LAP will decrease. Fig. 7a depicts the obviously reduced fluorescence intensities of LAP in HeLa cells incubated with WP5-NTA/MN after light irradiation, revealing that WP5-NTA/MN can still generate $ONOO^-$ in tumor cells.

Subsequently, the therapeutic performance of WP5-NTA/MN was investigated. Before evaluating its therapeutic ability, the biocompatibility of WP5-NTA/MN was first explored. Fig. 7b depicts the viability data for normal cells (HL-7702 cell) incubated with WP5-NTA/MN under different conditions. It can be concluded that WP5-NTA/MN shows no toxicity towards HL-7702 cells with or without light. Hemolysis tests were also conducted. As shown in Fig. S10 (ESI†), both low and high concentrations of the nanodrugs showed low hemolysis values. These results fully demonstrate that WP5-NTA/MN has excellent biocompatibility in completing tumor treatment.

Then the lethality values of WP5-NTA/MN towards HeLa cells were obtained using MTT assay. In the dark, WP5-NTA/MN cannot kill tumor cells, suggesting the negligible dark toxicity of WP5-NTA/MN (Fig. 7c). However, after exposure to white light (25 mW cm^{-2}), the lowest cell viability was about 20% (Fig. 7c). The therapeutic ability of WP5-NTA/MN was also confirmed by Calcein-AM/PI staining imaging of HeLa cells (Fig. S11, ESI†). In order to prove that the therapeutic ability of WP5-NTA/MN can be attributed to the combination of NO therapy and photodynamic therapy, the lethality values of NO therapy alone and PDT alone were obtained. These control experiments were carried out by incubating NO and ROS scavengers with cells (Figs. S12a and b, ESI†). As shown in Fig. S12c (ESI†), no treatment method alone can completely kill cancer cells, and the viability data of cells receiving one treatment mode alone are all above a half. WP5-NTA/MN can undergo O_2-insensitive type I PDT and NO therapy, therefore, it is expected that WP5-NTA/MN will also perform well in hypoxic cells. The viability values and the staining imaging of HeLa cells after receiving WP5-NTA/MN plus irradiation fully confirmed this hypothesis (Fig. 7d and Fig. S11, ESI†).

Inspired by its excellent performance *in vitro*, we immediately evaluated the therapeutic efficacy of WP5-NTA/MN *in vivo*. Fig. 8a depicts the experimental process *in vivo*. After the tumor grew to about 80 mm^3, the mice were randomly divided into four groups with three mice in each group. Two groups of mice were intravenously injected with PBS, and the other two groups

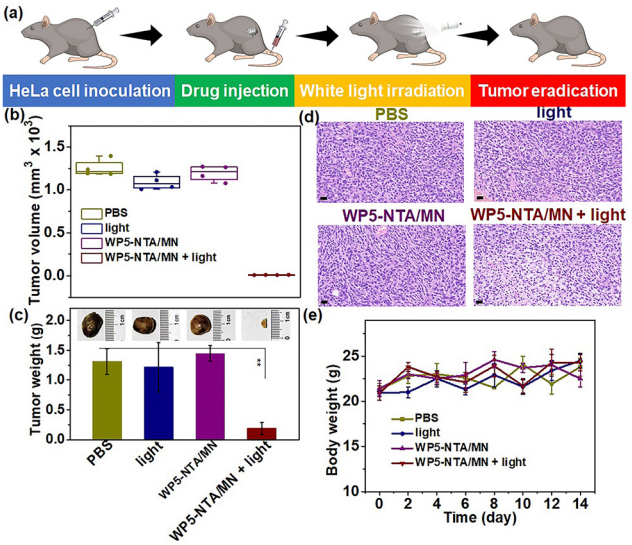

Fig. 8 (a) Illustration of the experimental process *in vivo*. (b) Tumor volumes from mice after receiving different treatments. (c) The average weights of tumors from mice receiving different treatments (inserted graph: tumors collected from the mice of different groups). $^{**}p < 0.01$. (d) H&E staining images of tumor slices from mice after receiving different treatments (scale bar: 20 μm). (e) The recorded body weight of mice in each group during treatments.

of mice were intravenously injected with WP5-NTA/MN. After 24 h, the two groups injected with PBS and WP5-NTA/MN were exposed to white light.

After 14 days of treatment, the tumor volume and weight of the mice in the different groups were recorded. As shown in Fig. 8b and c, the tumor sizes of mice receiving normal treatments were obviously smaller than those of mice in the control groups, which demonstrated that WP5-NTA/MN displayed excellent ability to inhibit tumor growth. Graphs of dissected tumors from mice after receiving different treatments also proved the good antitumor effects of the irradiated WP5-NTA/MN. During the treatments, the weights of the mice were monitored (Fig. 8e). All the mice retained similar body weights during the entire treatments, suggesting the good biosafety of WP5-NTA/MN to complete tumor therapy. Furthermore, based on their H&E staining images (Fig. S13, ESI†), no obvious damage was found in the main organs dissected from the mice after receiving the normal treatments, which also provided solid evidence for the excellent biosafety of WP5-NTA/MN. The values of parameters, values including WBC, RBC, HCT, HGB, MCH, MCHC, MCV and PLT, for all the mice were obtained during routine examination (Fig. S14, ESI†). It can be seen that none of the parameters of the mice in each group displayed significant differences, again indicating the absolute safety of WP5-NTA/MN.

Conclusions

In brief, through the integration of a subtly designed NO donor, **NTA-CN**, and type I photosensitizer, **DMATPE-MN**, an NO and type I PDT synergistic therapeutic system was constructed. Under single white light irradiation, **NTA-CN** can generate NO

radicals and **DMATPE-MN** exhibited excellent ability to generate $O_2^{\bullet-}$. Then, an amphiphilic pillararene, **WP5-PEG-OH**, was used to provide a powerful tool to integrate them *via* different noncovalent interactions. As expected, under white light irradiation, the formed nanodrug WP5-NTA/MN can generate $ONOO^-$ to achieve synergistic therapy. As a result, WP5-NTA/MN showed excellent therapeutic effects on HeLa cells in both normoxic and hypoxic microenvironments, while it showed no lethality against normal cells, suggesting its good biocompatibility. The experimental results *in vivo* proved again the superior antitumor effects and biosafety of WP5-NTA/MN. Therefore, this work provides a valuable multimodal synergistic therapy nanoplatform to achieve highly efficient tumor therapy, displaying great potential for practical clinical application.

Conflicts of interest

There are no conflicts to declare

Data availability

Data for this article are available in the Main Article and ESI.†

Acknowledgements

This work was supported by the National Natural Science Foundation of China (32301184), the Universities Natural Science Research Project of Jiangsu Province (23KJB150027) and the Large Instruments Open Foundation of Nantong University (KFJN2448).

Notes and references

1 R. L. Siegel, T. B. Kratzer, A. N. Giaquinto, H. Sung and A. Jemal, Cancer statistics, *CA Cancer J. Clin.*, 2025, **75**, 10–45.
2 C. Y. Tsang and Y. Zhang, Nanomaterials for light-mediated therapeutics in deep tissue, *Chem. Soc. Rev.*, 2024, **53**, 2898–2931.
3 C. Parisi, F. Laneri, A. Fraix and S. Sortino, Multifunctional Molecular Hybrids Photoreleasing Nitric Oxide: Advantages, Pitfalls, and Opportunities, *J. Med. Chem.*, 2024, **67**, 16932–16950.
4 X. Zhao, J. Liu, J. Fan, H. Chao and X. Peng, Recent Progress in Photosensitizers for Overcoming the Challenges of Photodynamic Therapy: from Molecular Design to Application, *Chem. Soc. Rev.*, 2021, **50**, 4185–4219.
5 X. Li, J. F. Lovell, J. Yoon and X. Chen, Clinical Development and Potential of Photothermal and Photodynamic Therapies for Cancer, *Nat. Rev. Clin. Oncol.*, 2020, **17**, 657–674.
6 Y. Wang, T. Yang and Q. He, Strategies for engineering advanced nanomedicines for gas therapy of cancer, *Natl. Sci. Rev.*, 2020, **7**, 1485–1512.
7 B. Lu, Y. Huang, H. Quan, Z. Zhang and Y. Yao, Organic Conjugated Small Molecules with Donor–Acceptor Structures: Design and Application in Phototherapy of Tumors, *Mater. Chem. Front.*, 2022, **6**, 2968–2993.
8 Z. Wang, A. Jin, Z. Yang and W. Huang, Advanced Nitric Oxide Generating Nanomedicine for Therapeutic Applications, *ACS Nano*, 2023, **17**, 8935–8965.
9 S. Liu, G. Li and D. Ma, Controllable Nitric Oxide-Delivering Platforms for Biomedical Applications, *Adv. Therap.*, 2022, **5**, 2100227.
10 X. Yuan, J.-L. Zhou, L. Yuan, J. Fan, J. Yoon, X.-B. Zhang, X. Peng and W. Tan, Phototherapy: progress, challenges, and opportunities, *Sci. China: Chem.*, 2025, **68**, 826–865.
11 X. Li, N. Kwon, T. Guo, Z. Liu and J. Yoon, Innovative Strategies for Hypoxic-Tumor Photodynamic Therapy, *Angew. Chem., Int. Ed.*, 2018, **57**, 11522–11531.
12 J. Chen, T. Fan, Z. Xie, Q. Zeng, P. Xue, T. Zheng, Y. Chen, X. Luo and H. Zhang, Advances in nanomaterials for photodynamic therapy applications: Status and challenges, *Biomaterials*, 2020, **237**, 119827.
13 G. Li, Q. Wang, J. Liu, M. Wu, H. Ji, Y. Qin, X. Zhou and L. Wu, Innovative strategies for enhanced tumor photodynamic therapy, *J. Mater. Chem. B*, 2021, **9**, 7347–7370.
14 Y. Wan, L.-H. Fu, C. Li, J. Lin and P. Huang, Conquering the Hypoxia Limitation for Photodynamic Therapy, *Adv. Mater.*, 2021, **33**, 2103978.
15 Y. Yang, Z. Huang and L.-L. Li, Advanced nitric oxide donors: chemical structure of NO drugs, NO nanomedicines and biomedical applications, *Nanoscale*, 2021, **13**, 444–459.
16 G. Li, L. Gu, C. Yang, X. Kong, Y. Qin and L. Wu, Lysosome-Anchoring Activation Design of Type I Photosensitizer Evokes Pyroptosis and Antitumor Immunity, *ACS Mater. Lett.*, 2024, **6**, 1820–1830.
17 B. Lu, H. Quan, Z. Zhang, T. Li, J. Wang, Y. Ding, Y. Wang, X. Zhan and Y. Yao, End Group Nonplanarization Enhances Phototherapy Efficacy of A–D–A Fused-Ring Photosensitizer for Tumor Phototherapy, *Nano Lett.*, 2023, **23**, 2831–2838.
18 B. Lu, J. Xia, H. Quan, Y. Huang, Z. Zhang and X. Zhan, End Group Engineering for Constructing A–D–A Fused-Ring Photosensitizers with Balanced Phototheranostics Performance, *Small*, 2024, **20**, 2307664.
19 D. Li, X. Chen, W. Dai, Q. Jin, D. Wang, J. Ji and B. Z. Tang, Photo-Triggered Cascade Therapy: A NIR-II AIE Luminogen Collaborating with Nitric Oxide Facilitates Efficient Collagen Depletion for Boosting Pancreatic Cancer Phototheranostics, *Adv. Mater.*, 2024, **36**, 2306476.
20 Y. Wang, X. Huang, Y. Tang, J. Zou, P. Wang, Y. Zhang, W. Si, W. Huang and X. Dong, A Light-induced Nitric Oxide Controllable Release Nano-platform based on Diketopyrrolopyrrole Derivatives for pH-responsive Photodynamic/photothermal Synergistic Cancer Therapy, *Chem. Sci.*, 2018, **9**, 8103–8109.
21 Y. Huang, Z. Wu, H. Wang, H. An, J. Zhang and Z. Bao, Nanogenerators with l-arginine loading: new choices as cascade and synergistic nitric oxide/photodynamic antitumor agents, *Mater. Chem. Front.*, 2025, **9**, 204–222.
22 A. Fraix and S. Sortino, Combination of PDT photosensitizers with NO photodononors, *Photochem. Photobiol. Sci.*, 2018, **17**, 533.

23 J. Zhu, W. Wang, X. Wang, L. Zhong, X. Song, W. Wang, Y. Zhao and X. Dong, Multishell Nanoparticles with Linkage Mechanism for Thermal Responsive Photodynamic and Gas Synergistic Therapy, *Adv. Healthcare Mater.*, 2021, **10**, 2002038.
24 H. Yin, X. Guan, H. Lin, Y. Pu, Y. Fang, W. Yue, B. Zhou, Q. Wang, Y. Chen and H. Xu, Nanomedicine-Enabled Photonic Thermogaseous Cancer Therapy, *Adv. Sci.*, 2020, **7**, 1901954.
25 J. Sun, X. Cai, C. Wang, K. Du, W. Chen, F. Feng and S. Wang, Cascade Reactions by Nitric Oxide and Hydrogen Radical for Anti-Hypoxia Photodynamic Therapy Using an Activatable Photosensitizer, *J. Am. Chem. Soc.*, 2021, **143**, 868–878.
26 S. Xie, C. Liu, Y. Cao, J. Xia and B. Lu, Pillararene based supramolecular nanoplatform for endoplasmic reticulum-targeting type I photodynamic and NO gas therapy, *Sci. China Mater.*, 2025, **68**, 1285–1291.
27 S. S. Wan, J. Y. Zeng, H. Cheng and X. Z. Zhang, ROS-induced NO generation for gas therapy and sensitizing photodynamic therapy of tumor, *Biomaterials*, 2018, **185**, 51–62.
28 C. Parisi, M. Failla, A. Fraix, L. Menilli, F. Moret, E. Reddi, B. Rolando, F. Spyrakis, L. Lazzarato, R. Fruttero, A. Gasco and S. Sortino, A generator of peroxynitrite activatable with red light, *Chem. Sci.*, 2021, **12**, 4740–4746.
29 D. Jiang, T. Yue, G. Wang, C. Wang, C. Chen, H. Cao and Y. Gao, Peroxynitrite ($ONOO^-$) generation from the HA-TPP@NORM nanoparticles based on synergistic interactions between nitric oxide and photodynamic therapies for elevating anticancer efficiency, *New J. Chem.*, 2020, **44**, 162–170.
30 N. V. Blough and O. C. Zafiriou, Reaction of superoxide with nitric oxide to form peroxonitrite in alkaline aqueous solution, *Inorg. Chem.*, 1985, **24**, 3502–3504.
31 C. Szabó, H. Ischiropoulos and R. Radi, Peroxynitrite: biochemistry, pathophysiology and development of therapeutics, *Nat. Rev. Drug Discovery*, 2007, **6**, 662–680.
32 W. Huang, J. Zhang, L. Luo, Y. Yu and T. Sun, Nitric Oxide and Tumors: From Small-Molecule Donor to Combination Therapy, *ACS Biomater. Sci. Eng.*, 2023, **9**, 139–152.
33 A. Mondal, S. Paul and P. De, Recent Advancements in Polymeric N-Nitrosamine-Based Nitric Oxide (NO) Donors and their Therapeutic Applications, *Biomacromolecules*, 2024, **25**, 5592–5608.
34 S. Sortino, S. Petralia, G. Compagnini, S. Conoci and G. Condorell, Light-Controlled Nitric Oxide Generation from a Novel Self-Assembled Monolayer on a Gold Surface, *Angew. Chem., Int. Ed.*, 2002, **41**, 1914–1916.
35 E. B. Caruso and S. Petralia, Sabrina Conoci, Salvatore Giuffrida and S. Sortino, Photodelivery of Nitric Oxide from Water-Soluble Platinum Nanoparticles, *J. Am. Chem. Soc.*, 2007, **129**, 480–481.
36 N. Kandoth, E. Vittorino, M. T. Sciortino, T. Parisi, I. Colao, A. Mazzaglia and S. Sortino, A Cyclodextrin-Based Nanoassembly with Bimodal Photodynamic Action, *Chem. Eur. J.*, 2012, **18**, 1684–1690.
37 N. Kandoth, V. Kirejev, S. Monti, R. Gref, M. B. Ericson and S. Sortino, Two-photon fluorescence imaging and bimodal phototherapy of epidermal cancer cells with biocompatible self-assembled polymer nanoparticles, *Biomacromolecules*, 2014, **15**, 1768–1776.
38 A. Fraix, N. Kandoth, I. Manet, V. Cardile, A. C. Graziano, R. Gref and S. Sortino, An engineered nanoplatform for bimodal anticancer phototherapy with dual-color fluorescence detection of sensitizers, *Chem. Commun.*, 2013, **49**, 4459–4461.
39 V. Rapozzi, D. Ragno, A. Guerrini, C. Ferroni, E. della Pietra, D. Cesselli, G. Castoria, M. Di Donato, E. Saracino, V. Benfenati and G. Varchi, Androgen Receptor Targeted Conjugate for Bimodal Photodynamic Therapy of Prostate Cancer in Vitro, *Bioconjug. Chem.*, 2015, **26**, 1662–1671.
40 A. Fraix, M. Blangetti, S. Guglielmo, L. Lazzarato, N. Marino, V. Cardile, A. C. Graziano, I. Manet, R. Fruttero, A. Gasco and S. Sortino, Light-Tunable Generation of Singlet Oxygen and Nitric Oxide with a Bichromophoric Molecular Hybrid: a Bimodal Approach to Killing Cancer Cells, *ChemMedChem*, 2016, **11**, 1371–1379.
41 B. Lu, Y. Huang, J. Xia and Y. Yao, Active targeted drug delivery system constructed from functionalized pillararenes for chemo/photodynamic synergistic therapy, *Front. Chem. Sci. Eng.*, 2024, **18**, 138.
42 B. Lu, J. Xia, Y. Huang and Y. Yao, The design strategy for pillararene based active targeted drug delivery systems, *Chem. Commun.*, 2023, **59**, 12091–12099.
43 X. Li, M. Shen, J. Yang, L. Liu and Y. W. Yang, Pillararene-Based Stimuli-Responsive Supramolecular Delivery Systems for Cancer Therapy, *Adv. Mater.*, 2024, **36**, 2313317.
44 H. Zhang and Y. Zhao, Pillararene-Based Assemblies: Design Principle, Preparation and Applications, *Chem. Eur. J.*, 2013, **19**, 16862–16879.
45 H. Zhu, Q. Li, L. E. Khalil-Cruz, N. M. Khashab, G. Yu and F. Huang, Pillararene-based supramolecular systems for theranostics and bioapplications, *Sci. China: Chem.*, 2021, **64**, 688–700.
46 H. Wang, Y. Wang, W. Xu, H. Zhang, J. Lv, X. Wang, Z. Zheng, Y. Zhao, L. Yu, Q. Yuan, L. Yu, B. Zheng and L. Gao, Host-Guest-Interaction Enhanced Nitric Oxide Photo-Generation within a Pillar[5]arene Cavity for Antibacterial Gas Therapy, *ACS Appl. Mater. Interfaces*, 2023, **15**, 54266–54279.
47 H. Zhang, J. Lv, X. Yang, B. Zheng and L. Gao, Pillar[5]arene stabilized gold nanoparticles for the enhanced light-triggered nitric oxide release with antibacterial and anti-biofilm activities, *Mater. Today Chem.*, 2024, **42**, 102377.
48 M. L. Hause, N. Herath, R. Zhu, M. C. Lin and A. G. Suits, Roaming-mediated isomerization in the photodissociation of nitrobenzene, *Nat. Chem.*, 2011, **3**, 932–937.
49 N. A. Lau, D. Ghosh, S. Bourne-Worster, R. Kumar, W. A. Whitaker, J. Heitland, J. A. Davies, G. Karras, I. P. Clark, G. M. Greetham, G. A. Worth, A. J. Orr-Ewing and H. H. Fielding, Unraveling the Ultrafast Photochemical Dynamics of Nitrobenzene in Aqueous Solution, *J. Am. Chem. Soc.*, 2024, **146**, 10407–10417.